

Comparing the atomic and macroscopic aging dynamics in an amorphous and partially crystalline $Zr_{44}Ti_{11}Ni_{10}Cu_{10}Be_{25}$ bulk metallic glass

Published in revised form at:

Journal of Materials Research Vol. 2 Num. 11 Pags: 2014-2021, 2017.

<https://doi.org/10.1557/jmr.2017.187>

Copyright holder (Materials Research Society)

Zach Evenson^{a,*}, Alba Payes-Playa^{b,c}, Yuriy Chushkin^b, Marco di Michiel^b, Eloi Pineda^d and Beatrice Ruta^{b,e*}

^a Heinz Maier-Leibnitz Zentrum (MLZ) and Physik Department, Technische Universität München, Lichtenbergstrasse 1, 85748 Garching, Germany.

^b ESRF – The European Synchrotron, CS 40220, 38043 Grenoble, France.

^c Universidad Autonoma de Madrid, Spain.

^d Departament de Física, Universitat Politècnica Catalunya - BarcelonaTech, ESAB, Esteve Terradas 8, 08860 Castelldefels, Spain.

^e Institute of Light and Matter, UMR5306 Université Lyon 1-CNRS, Université de Lyon, 69622 Villeurbanne Cedex, France.

*Corresponding authors:

zachary.evanson@frm2.tum.de

beatrice.ruta@univ-lyon1.fr

ABSTRACT

Several recent x-ray photon correlation spectroscopy works have reported an anomalous atomic dynamics in hyper-quenched metallic glasses. Here, we compare and contrast these microscopic dynamics with that found in a $\text{Zr}_{44}\text{Ti}_{11}\text{Ni}_{10}\text{Cu}_{10}\text{Be}_{25}$ bulk metallic glass, prepared with a cooling rate some 6 orders of magnitude lower. In both cases, structural relaxation in the glass is governed by internal stresses, giving rise to highly compressed density correlation functions. Differently from the fast aging reported in previous studies, here the atomic dynamics displays a slow linear atomic-level aging, while not affecting the shape parameter. Traditional macroscopic phenomenological models fail to capture the temperature dependence of the microscopic structural relaxation time, suggesting a length scale dependence of the aging. Interestingly, the dynamics does not seem to be affected by the presence of a low percentage of frozen in nanocrystals and displays a temperature dependence similar to that observed in macroscopic viscosity measurements.

I. INTRODUCTION

The nature of the glassy state continues to stimulate broad discussion throughout the physics and materials science communities.¹⁻³ Glasses are in an out-of-equilibrium state and their properties will evolve with time back towards the equilibrium liquid below the glass transition temperature T_g . This is the phenomenon of physical aging, which is an important – and often altogether unavoidable – component of practical design and application of technologically relevant amorphous materials,⁴ in particular bulk metallic glasses (BMGs).⁵⁻⁷

In recent years, x-ray photon correlation spectroscopy (XPCS) has provided an unprecedented look into the aging dynamics of metallic glasses directly on the atomic length scale.⁸⁻¹³ The existence of distinct structural rearrangements far below T_g ,⁸ compressed exponential relaxation functions¹⁰ and intermittent aging dynamics¹¹ all suggest a complex microscopic picture of metallic glass aging, not reflected in measurements of bulk macroscopic quantities.¹⁴⁻¹⁶ Here we investigate the microscopic dynamics in the $Zr_{44}Ti_{11}Ni_{10}Cu_{10}Be_{25}$ (Vitreloy 1b) BMG. In particular, we present some intriguing features of the atomic-scale structural relaxation, as revealed by state-of-the-art XPCS techniques, and compare and contrast them to previously investigated simple and glass-forming metallic systems. Additionally, we show that, in the present case, a small volume fraction of frozen-in nanocrystals does not seem to affect the overall microscopic dynamics, which is governed by a linear scaling law, in contrast to the fast exponential growth observed in hyper-quenched ribbons.^{8,10}

II. EXPERIMENTAL

The $Zr_{44}Ti_{11}Ni_{10}Cu_{10}Be_{25}$ alloy was chosen for these experiments, as it does not show phase separation in the vicinity of T_g , which is known to significantly affect the observed aging behavior during long-time annealing.¹⁷⁻¹⁹ Additionally, comprehensive measurements of enthalpy recovery, volume and viscosity during aging of this composition have been carried out previously,¹⁶ allowing for a detailed comparison of microscopic and bulk macroscopic properties. Amorphous rods of $Zr_{44}Ti_{11}Ni_{10}Cu_{10}Be_{25}$ were supplied by Liquidmetal[®] Technologies. The cooling rate of the rod is estimated to be 10-50 K/s.^{17,20} Differential scanning calorimetry experiments¹⁶ have determined a $T_g = 620$ K at a heating rate of 25 K/min.

Dynamic mechanical analysis (DMA) of melt-spun ribbons was performed in tensile geometry in a TA Instruments Q800 DMA. Multi-frequency tests (frequencies of 0.3, 1, 3, 10 and 30 Hz) were carried out at a constant heating rate of 1 K/min from ambient temperature up to 823 K. An oscillating strain of 0.5 μm amplitude was applied to samples with lengths of 15 mm under a static pre-load tension of 0.06 N. The dependence of the α -relaxation time τ_α on temperature was calculated from the position of the main relaxation peak at each frequency.

The XPCS measurements were performed at the beamline ID10 at ESRF, France. A partially coherent beam with an energy of 8.1 keV was selected by a Si(1,1,1) monochromator and focused onto the sample through beryllium compound refractive lenses. The coherent part of the beam was defined by rollerblade slits closed $10 \times 10 \mu m$. Series of speckles patterns were collected in transmission geometry by a charge-coupled-device (CCD) from Andor technology ($13 \times 13 \mu m$ pixel size) placed ~ 70 cm downstream of the sample at an angle $2\theta \sim 40^\circ$, corresponding to the maximum of the first sharp diffraction peak of the amorphous alloy. The raw data were treated as in Ref.²¹

A resistively heated furnace with a temperature stability better than 0.1 K was used to heat and cool the sample under high vacuum conditions. For the XPCS measurements, samples of $\text{Zr}_{44}\text{Ti}_{11}\text{Ni}_{10}\text{Cu}_{10}\text{Be}_{25}$ were obtained from a piece of a water-quenched bulk glassy rod of 10 mm in diameter via diamond saw cutting and then mechanically polished down to $\sim 60 \mu\text{m}$. Structural analysis of the investigated samples was carried out at the beamline ID15 at ESRF, with an incident wavelength $\lambda=0.1425 \text{ \AA}$. The data were collected with a 2D Pixium detector located far from the sample in order to highlight the low momentum transfer (q) range of interest in the XPCS measurements.

III. RESULTS AND DISCUSSION

For the XPCS measurements, the initially glassy sample was annealed above T_g at 633 K for ~ 60 min, which induced the formation of nanocrystals. The diffracted intensities of both the completely amorphous and partially crystalline samples obtained in XRD measurements at ambient temperature are given in Fig. 1. As both samples were measured under the same experimental conditions, we can estimate the crystalline volume fraction by scaling the amorphous pattern onto the crystalline one in the q regions far from the Bragg peaks where the signal is thus dominated by the amorphous component. This procedure gives a crystalline volume fraction of 5%. This amount was found to do not evolve additionally once the system was cooled back below T_g during the XPCS measurements. By slowly step-cooling back into the glass with a rate of 1 K/min, we thus investigate the effect of this small fraction of frozen in nanocrystals on the atomic scale aging dynamics during each isothermal hold. These data have been compared with additional measurements taken in a fully amorphous sample, by step-heating the glass from room temperature. In both samples, the

dynamics was measured in isothermal conditions for ~ 5 hr, thus allowing us to also follow the temporal evolution of the atomic motion.

The microscopic dynamics is accessed in XPCS through a one-time intensity auto-correlation function $g_2(q,t)$, which is directly related to the decay of density fluctuations in the glass on a microscopic length scale given by the probed q -value via the Siegert relation

$$g_2(q,t) = 1 + \gamma |\Phi(q,t)|^2, \quad (1)$$

where γ is the experimental speckle contrast and $\Phi(q,t) = S(q,t)/S(q,0)$ is the normalized density correlation function.²² By performing measurements at $q = q_0$, the first maximum in the static structure factor $S(q)$, the microscopic dynamics is probed on a length scale of $2\pi/q_0 \sim 2 \text{ \AA}$, corresponding to the average atomic nearest-neighbor separation in the glass. Since $q_0 = 2.6 \text{ \AA}^{-1}$ is situated between the two primary crystalline peaks indicated in Fig. 1, the scattered intensity is homogeneously distributed over the CCD detector. Hence, we were able to calculate the standard $g_2(q_0,t)$ and indeed observe the effect of prior nanocrystallization on the atomic dynamics in the glass.

We model the decay of $g_2(q_0,t)$ using a Kohlrausch-Williams-Watts (KWW) expression^{23,24}

$$g_2(q_0,t) = 1 + c \exp\left[-2(t/\tau)^\beta\right], \quad (2)$$

where τ is the relaxation time, β is the shape parameter, and $c = \gamma f_q^2$ is the product between the experimental contrast γ and the square of the Debye-Waller factor f_q . For $T \leq 603$ K, the

atomic dynamics of the glass slows down enough to be explored by the time window accessible in XPCS; i.e., $\tau \gtrsim 100$ s. In Fig. 2(a) we show the temperature dependence of $g_2(q_0, t)$ of the partially crystallized sample taken at a constant waiting time $t_w = 7 \times 10^3$ s from temperature equilibration, along with best fits to Eq. (2).

As is evident in Fig. 2(a), the decay of $g_2(q_0, t)$ shifts to longer times upon lowering the temperature, a simple consequence of the decrease of thermal motion and increase in τ . The shape of $g_2(q_0, t)$ in the glassy state is well described by a compressed exponential decay [Eq. (2)] with a $\beta > 1$, which appears to systematically decrease with proximity to T_g (~ 620 K) [Fig. 2(b)]. While stretched exponential functions ($\beta < 1$) are commonly observed in a wide range of glassy relaxation phenomena and have been attributed to an underlying dynamical heterogeneity,²⁵ compressed exponentials, on the other hand, are indicative of a microscopic dynamics governed by the presence of internal stresses and cannot be rationalized within the heterogeneous dynamics scenario.^{26,27} In fact, **theoretical and simulation studies suggest that long-range anisotropic stresses arising from dipole forces are integral to understanding aging in disordered matter.**^{28,29} Even in the deeply supercooled liquid state, there are indications that the relaxation dynamics can be described through an accumulation of Eshelby transformations; i.e., local structural rearrangements resulting in long-range stress fluctuations and elastic strains^{30,31}. In this sense, the compressed form of the exponential relaxation function of metallic glasses probed in XPCS might also result from a series of such Eshelby transformations, each contributing a Debye term with a well-defined relaxation time. In order to reproduce an apparent compressed exponential form, however, the contribution of some of these processes must have an opposite sign than the others. So far, we are unaware of any work that has thus far provided a direct link between Eshelby events and aging in metallic glasses, although recent studies have highlighted the important role played by atomic-level stresses.^{11,13,32} The decrease in β near T_g reflects the system's close proximity to its

equilibrium state (supercooled liquid), where the microscopic dynamics is indeed characterized by stretched exponential correlation functions, in accord with a heterogeneous dynamics scenario.^{33–35} Upon cooling from the liquid, β increases smoothly and becomes constant, suggesting a continuous evolution from the supercooled liquid to the glassy state.⁸

In a different experimental protocol, a fully amorphous sample of $\text{Zr}_{44}\text{Ti}_{11}\text{Ni}_{10}\text{Cu}_{10}\text{Be}_{25}$ was investigated by step-heating from the glassy state up to 495 K. Unfortunately, due to experimental constraints relating to available beam time, the temperature interval of ~ 40 K between these two samples was not investigated. However, it would appear that, at least within the fitting uncertainty, the values of β obtained in both sets of measurements remain comparable and temperature independent in a certain temperature regime below T_g , despite the different structural state of the sample and asymmetric thermal protocols employed. At the lowest investigated temperature of 345 K (not shown), β has a value of 2.0 ± 0.1 . A noticeable decrease to $\beta = 1.5 \pm 0.1$ is observed during heating between 455 and 475 K [Fig. 2(b)], which is in line with previous experimental findings and has been related to the decrease in atomic-level stresses.^{8,10} It should be noted that this temperature range also corresponds to that of the fast β -relaxation observed in DMA studies on a similar $\text{Zr}_{46.25}\text{Ti}_{8.25}\text{Cu}_{7.5}\text{Ni}_{10}\text{Be}_{27.5}$ (Vitreloy 4) alloy.³⁶ Thus, the decrease in β observed in this temperature range might also be connected to the low-temperature onset of stress relaxation and excess free volume annihilation in the glassy state.¹²

To investigate the changes to the atomic motion as a result of aging, we compare the waiting time-dependent dynamics in the partially crystallized sample close to T_g with that in the fully amorphous sample measured during step-heating from ambient temperature. This will allow us to confirm whether the microscopic dynamics indeed behaves qualitatively similar, given the presence of a small percentage of nanocrystals. Between 475 and 583 K, all

$g_2(q_0, t)$ curves obey a common time-temperature-waiting time superposition – regardless of thermal history – with a $\langle\beta\rangle = 1.5$, shown as master curves in Fig. 3.

Figure 4 shows the evolution of τ as a function of t_w . To compare the aging dynamics at different temperatures, we normalize the data by a common initial value $\tau_I(T)$. Firstly, it is apparent that, at all temperatures below 598 K, τ follows a linear scaling such that $\tau(T, t_w)/\tau_I(T) \propto t_w$. In contrast to this, a fast exponential growth of τ has been observed in similar XPCS studies on hyper-quenched metallic glass ribbons,^{8,10} which has been related to the large amount of free volume and, hence, internal stresses¹³ produced by the extremely fast quenching rates of $\sim 10^6$ K/s. This would thus suggest that the linear growth in τ observed here is simply a result of the much lower cooling rate used to produce these bulk samples. An alternative explanation could, however, reside in the different nature of the probed system. Short-time exponential aging has been reported for 2 and 3-component metallic glasses – systems with less dense atomic packing than the $Zr_{44}Ti_{11}Ni_{10}Cu_{10}Be_{25}$ alloy measured in this work. Hence, the linear atomic aging reported here could be a consequence of this system's better ability at **avoiding thermally-induced microscopic stresses** while cooling from the high-temperature melt during the sample preparation. The fact that the τ measured upon slow cooling from the supercooled liquid scale in an identical fashion to those measured in the as-quenched BMG would seem to support this hypothesis. This is also consistent with the faster evolution of τ and larger value of β observed in the data taken at the lowest temperature (345 K), where the as-cast BMG sample has the largest amount of free volume and, accordingly, greatest degree of internal stresses. Here, we recall that in-situ aging is expected during the long isothermal steps of the XPCS measurements and, therefore, the glass measured at the higher temperature steps has already released part of the excess free-volume and internal stresses frozen-in of the initial as-quenched samples. The analysis in Fig. 4 thus shows that, even if the sample is partially crystalline, the microscopic aging of the system is obviously

still governed by the amorphous matrix, and the presence of 5% of frozen in nanocrystals has negligible impact on the atomic dynamics probed using XPCS.

At the highest investigated temperature (598 K) τ apparently displays no dependence on t_w within the experimental time scale, despite the sample still being in the glassy state, as evidenced by a $\beta > 1$ [Fig. 2(b)]. A similar stationary dynamics close to T_g was reported in recent XPCS studies on the $\text{Pd}_{43}\text{Cu}_{27}\text{Ni}_{10}\text{P}_{20}$ BMG¹¹ and also observed at low temperatures in hyper-quenched metallic glass ribbons subjected to long annealing times.^{8,10} This crossover into a stationary dynamics regime and subsequent lack of aging in metallic glasses on the atomic length scale is a result of configurational changes to the glassy structure, which run independently of macroscopic density changes.¹³ Within the energy landscape picture,^{37,38} this can be interpreted as the system being trapped in a local minimum of a potential energy basin, where it is nevertheless able to explore a local region of its configuration space, hence the full decay of $g_2(q_0, t)$ within the experimental time window. This type of localized dynamics in metallic glasses has been explored in recent simulation work.³²

Lastly, in order to highlight the deviation of the microscopic dynamics from the expected evolution of the macroscopic τ , we apply a nonlinear relaxation model based on the Tool-Narayanaswamy-Moynihan (TNM) formalism³⁹⁻⁴¹ and compare sets of data taken using a range of macroscopic relaxation techniques with those obtained here using XPCS.

The values of τ for $\text{Zr}_{44}\text{Ti}_{11}\text{Ni}_{10}\text{Cu}_{10}\text{Be}_{25}$ determined in the vicinity of T_g are plotted in Fig. 5 as a function of inverse temperature. The filled circles are the results of DMA measurements and correspond to the temperature at which τ_α is equal to the inverse of the applied test frequency, namely $\tau_\alpha = 1/\omega$. The filled square and filled triangle symbols were

taken from equilibrium and non-equilibrium viscosities, respectively, determined in isothermal annealing experiments below T_g using a three-point bending-method.¹⁶

In order to calculate τ from the reported viscosity values, we use the Maxwell relation⁴²

$$\eta = \tau G_\infty \quad (3)$$

where G_∞ is the high-frequency shear modulus. The value of $G_\infty = 34.52$ GPa was determined for the similar Vitreloy 4 alloy near its calorimetric T_g .^{43,44} The measured value of G_∞ for metallic glasses not only depends on the temperature, but also on t_w and thermal history of the sample.⁴³⁻⁴⁵ In general, we estimate that these effects would increase G_∞ by a maximum of around 10 % at the lowest investigated temperatures. This uncertainty has been incorporated into our analysis; however, it is well within the error bars of the viscosity values reported in Ref.¹⁶

The values of τ measured at $t_w = 7 \times 10^3$ s using XPCS (open triangles) are given alongside those calculated from glassy state viscosities using beam-bending (filled triangles) in Fig. 5. The departure from equilibrium occurs at a lower temperature in the XPCS experiments due to the quasi-static cooling rate of 1 K/min, in contrast to the heating rate of 25 K/min employed in the beam-bending experiments.¹⁶ Notwithstanding, the values of τ obtained in XPCS clearly display a similar temperature dependence as the macroscopic data, despite the presence of a small nanocrystalline volume fraction.

The temperature dependence of all equilibrium τ is very well described over the data range of some 6 orders of magnitude with the empirical Vogel-Fulcher-Tammann (VFT) equation⁴⁶⁻⁴⁸

$$\tau(T) = \tau_0 \exp\left(\frac{D^* T_0}{T - T_0}\right). \quad (4)$$

Keeping the value of τ_0 fixed at 1×10^{-14} s, we obtain the fitting parameters $D^* = 25.4 \pm 1.4$ and $T_0 = 358.2 \pm 8.2$ K. The fitted curve is given by the dashed line in Fig. 5.

Using the TNM model, the evolution of the fictive temperature³⁹ T_f is calculated as

$$T_f(T, t) = T - \int_{T_{eq}}^T dT' \exp\left[-\left(\int_{T'}^T \frac{dT''}{\dot{T} \tau(T, T_f)}\right)^\beta\right], \quad (5)$$

where T_{eq} is the starting T in equilibrium and $\dot{T} = dT/dt$ is the heating/cooling rate. In this model, the structural relaxation kinetics are assumed to follow a KWW form $\sim \exp\left[-(t/\tau)^{\beta_{TNM}}\right]$. The shape parameter β_{TNM} in this case characterizes the width of the distribution of τ and, as such, $0 < \beta_{TNM} \leq 1$. The above model assumes validity of the time-temperature-superposition principle, requiring β_{TNM} to be a constant in the temperature range of interest. Using the empirical relations established by Vilgis⁴⁹ and Böhmer et al.,⁵⁰ the KWW shape parameter is related to the VFT parameters via $\beta = 1 - \sqrt{(T_0/T_g)^2 / D^*}$. For $Zr_{44}Ti_{11}Ni_{10}Cu_{10}Be_{25}$ this results in a $\beta_{TNM} = 0.88$, in good agreement with what is found in the equilibrium melt of similar compositions using quasi-elastic neutron scattering.³³⁻³⁵

Various phenomenological equations have been used to describe the dependence of τ on both T and T_f .⁵¹ Here we employ a form of the equation derived by Scherer⁵² and Hodge,⁵³

$$\tau(T, T_f) = \tau_0 \exp\left[\frac{D^* T_0}{T(1 - T_0/T_f)}\right], \quad (6)$$

where the parameters τ_0 , D^* and T_0 are the same as in Eq. (4). It can be easily verified that the above expression reduces to Eq. (4) in the equilibrium case where $T_f = T$.

The solid curve in Fig 5 shows the expected evolution of τ calculated from Eqs. (5) and (6) according to the isothermal holding times and temperatures of our XPCS experiments. It is evident that, after departure from the equilibrium state, the TNM model predicts values of τ up to at least an order of magnitude larger than what is experimentally observed in XPCS. Moreover, the model clearly shows a return to equilibrium within the time scale of each isothermal hold, while the experimental XPCS data follow a temperature dependence indicative of the glassy state, as if little or no aging had taken place. This shows that, at least with our chosen set of input parameters, the TNM model fails to reproduce the evolution of the microscopic τ measured using XPCS and suggests the existence of a completely different mechanism of relaxation occurring at the atomic level. Similar results were also recently obtained during XPCS studies on a network-forming sodium silicate glass.⁵⁴

The TNM and similar phenomenological models have had broad success in describing many aspects of structural relaxation in amorphous materials, although their inadequacies have also been well documented.^{40,41,51,55–58} In the case of the XPCS experiments performed here, the failure of the TNM model is essentially due to the basic assumption that τ depends on the instantaneous state of the material via T_f . This is an over-simplification as it considers

that a given glassy configuration can be defined by a single parameter like T_f or some macroscopic variable like specific volume or enthalpy and does not explicitly incorporate any microscopic details of the system under investigation. Thus, the unique out-of-equilibrium phenomena revealed by XPCS, such as an absence of atomic-level aging, compressed correlation functions and stress-dominated dynamics, are not captured in these numerical models, or in any current theory of the glassy state for that matter.

IV. CONCLUSION

We have investigated the atomic aging dynamics in partially crystallized and fully amorphous specimens of the $Zr_{44}Ti_{11}Ni_{10}Cu_{10}Be_{25}$ bulk metallic glass using x-ray photon correlation spectroscopy. The microscopic dynamics in the two samples is characterized by a compressed decay of the intensity auto-correlation function and dominated by atomic-level stresses introduced during the formation of the glass. The structural relaxation in both samples exhibits a roughly constant shape factor $\langle\beta\rangle \sim 1.5$ and a time-temperature-waiting time superposition was found to hold, despite the asymmetry in thermal protocols. We have furthermore shown that the presence of approximately 5 % frozen in nanocrystals has no discernible effect on the microscopic dynamics, and that the temperature dependence of the τ measured in XPCS is in agreement with macroscopic viscosity data of the glass.

For almost all temperatures, τ was found to increase linearly with t_w , in contrast to the fast exponential growth observed in hyper-quenched metallic glass ribbons. This is likely an effect of the lower degree of atomic-level stresses, due to the orders of magnitude lower cooling rate used to produce the BMG specimen and to the multi-component nature of the system. A regime of stationary dynamics was discovered in the vicinity of T_g , where no apparent dependence of τ on t_w was observed, reminiscent of the equilibrium state of the supercooled

liquid, also marked by the lower value of the shape exponent $\beta \approx 1$. Finally, we have shown that the microscopic τ evolve in the glassy state completely differently than what is expected from the TNM model. This result confirms that the microscopic and macroscopic aging apparently obey different mechanisms and a more detailed investigation of this discrepancy is currently underway.

Acknowledgements

The authors would like to thank Ralf Busch for the use of the laboratory facilities to prepare the XPCS samples and Andy Waniuk for providing the sample material. ESRF is gratefully thanked for financing support of the stay of A. Payes-Playa at beamline ID10. We would also like to thank Referee #1 for their insightful comments on the compressed exponential during the review stage of this manuscript

1. V. Lubchenko and P. G. Wolynes: Theory of aging in structural glasses. *J. Chem. Phys.* **121**(7), 2852 (2004).
2. L. Berthier and G. Biroli: Theoretical perspective on the glass transition and amorphous materials. *Rev. Mod. Phys.* **83**(2), 587 (2011).
3. J. Zhao, S. L. Simon, and G. B. McKenna: Using 20-million-year-old amber to test the super-Arrhenius behaviour of glass-forming systems. *Nat. Commun.* **4**, 1783 (2013).
4. J. C. Mauro, D. Allan, and M. Potuzak: Nonequilibrium viscosity of glass. *Phys. Rev. B* **80**(9), 1 (2009).
5. M. E. Launey, R. Busch, and J. J. Kruzic: Influence of structural relaxation on the fatigue behavior of a ZrTiNiCuBe bulk amorphous alloy. *Scr. Mater.* **54**, 483 (2006).
6. Z. Evenson, T. Koschine, S. Wei, O. Gross, J. Bednarcik, I. Gallino, J. J. Kruzic, K.

- Rätzke, F. Faupel, and R. Busch: The effect of low-temperature structural relaxation on free volume and chemical short-range ordering in a Au₄₉Cu_{26.9}Si_{16.3}Ag_{5.5}Pd_{2.3} bulk metallic glass. *Scr. Mater.* **103**, 14 (2015).
7. Z. Evenson, S. E. Naleway, S. Wei, O. Gross, J. J. Kruzic, I. Gallino, W. Possart, M. Stommel, and R. Busch: β relaxation and low-temperature aging in a Au-based bulk metallic glass: From elastic properties to atomic-scale structure. *Phys. Rev. B* **89**(17), 174204 (2014).
 8. B. Ruta, Y. Chushkin, G. Monaco, L. Cipelletti, E. Pineda, P. Bruna, V. M. Giordano, and M. Gonzalez-Silveira: Atomic-Scale Relaxation Dynamics and Aging in a Metallic Glass Probed by X-Ray Photon Correlation Spectroscopy. *Phys. Rev. Lett.* **109**(16), 165701 (2012).
 9. M. Leitner, B. Sepiol, L.-M. Stadler, and B. Pfau: Time-resolved study of the crystallization dynamics in a metallic glass. *Phys. Rev. B* **86**(6), 64202 (2012).
 10. B. Ruta, G. Baldi, G. Monaco, and Y. Chushkin: Compressed correlation functions and fast aging dynamics in metallic glasses. *J. Chem. Phys.* **138**(5), 54508 (2013).
 11. Z. Evenson, B. Ruta, S. Hechler, M. Stolpe, E. Pineda, I. Gallino, and R. Busch: X-Ray Photon Correlation Spectroscopy Reveals Intermittent Aging Dynamics in a Metallic Glass. *Phys. Rev. Lett.* **115**(17), 175701 (2015).
 12. X. D. Wang, B. Ruta, L. H. Xiong, D. W. Zhang, Y. Chushkin, H. W. Sheng, H. B. Lou, Q. P. Cao, and J. Z. Jiang: Free-volume dependent atomic dynamics in beta relaxation pronounced La-based metallic glasses. *Acta Mater.* **99**, 290 (2015).
 13. V. M. Giordano and B. Ruta: Unveiling the structural arrangements responsible for the atomic dynamics in metallic glasses during physical aging. *Nat. Commun.* **7**, 1 (2015).
 14. S. Radelaar and A. van den Beukel: On the kinetics of structural relaxation in metallic glasses. *Acta Metall.* **31**(3), 419 (1983).
 15. A. Slipenyuk and J. Eckert: Correlation between enthalpy change and free volume

- reduction during structural relaxation of Zr₅₅Cu₃₀Al₁₀Ni₅ metallic glass. *Scr. Mater.* **50**(1), 39 (2004).
16. Z. Evenson and R. Busch: Equilibrium viscosity, enthalpy recovery and free volume relaxation in a Zr₄₄Ti₁₁Ni₁₀Cu₁₀Be₂₅ bulk metallic glass. *Acta Mater.* **59**, 4404 (2011).
 17. T. A. Waniuk, R. Busch, A. Masuhr, and W. L. Johnson: Viscosity of the Zr_{41.2}Ti_{13.8}Cu_{12.5}Ni₁₀Be_{22.5} bulk metallic glass-forming liquid and viscous flow during relaxation, phase separation, and primary crystallization. *Acta Mater.* **46**(15), 5229 (1998).
 18. C. C. Hays, C. P. Kim, and W. L. Johnson: Large supercooled liquid region and phase separation in the Zr-Ti-Ni- Cu-Be bulk metallic glasses. *Appl. Phys. Lett.* **75**(8), 1089 (1999).
 19. Z. Evenson, S. Raedersdorf, I. Gallino, and R. Busch: Equilibrium viscosity of Zr-Cu-Ni-Al-Nb bulk metallic glasses. *Scr. Mater.* **63**, 573 (2010).
 20. T. A. Waniuk: Viscosity and Crystallization in a Series of Zr-Based Bulk Amorphous Alloys Thesis by Andy Waniuk, California Institute of Technology, 2004.
 21. Y. Chushkin, C. Caronna, and A. Madsen: A novel event correlation scheme for X-ray photon correlation spectroscopy. *J. Appl. Crystallogr.* **45**(4), 807 (2012).
 22. A. Madsen, A. Fluerasu, and B. Ruta: in *Synchrotron Light Sources Free. Lasers* (Springer, 2014), pp. 1–21.
 23. R. Kohlrausch: Theorie des elektrischen Rückstandes in der Leidner Flasche. *Ann. der Phys. und Chemie* **91**(56–82), 179 (1854).
 24. G. Williams and C. Watts: Non-Symmetrical Dielectric Relaxation Behaviour Arising from a Simple Empirical Decay Function. *Trans. Faraday Soc.* **66**, 80 (1970).
 25. M. D. Ediger: Spatially heterogeneous dynamics in supercooled liquids. *Annu. Rev. Phys. Chem.* **51**, 99 (2000).

26. J.-P. Bouchaud and E. Pitard: Anomalous dynamical light scattering in soft glassy gels. *Eur. Phys. J. E* **6**, 231 (2001).
27. L. Cipelletti, L. Ramos, S. Manley, E. Pitard, D. A. Weitz, E. E. Pashkovski, and M. Johansson: Universal non-diffusive slow dynamics in aging soft matter. *Faraday Discuss.* **123**, 237 (2003).
28. E. E. Ferrero, K. Martens, and J.-L. Barrat: Relaxation in yield stress systems through elastically interacting activated events. *Phys. Rev. Lett.* **113**(24), 248301 (2014).
29. P. Chaudhuri and L. Berthier: Ultra-long-range dynamic correlations in a microscopic model for aging gels. *arXiv* 1 (2016).
30. A. Lemaître: Structural relaxation is a scale-free process. *Phys. Rev. Lett.* **113**, 245702 (2014).
31. A. Lemaître: Tensorial analysis of Eshelby stresses in 3D supercooled liquids. *J. Chem. Phys.* **143**, 164515 (2015).
32. Y. Fan, T. Iwashita, and T. Egami: Crossover from Localized to Cascade Relaxations in Metallic Glasses. *Phys. Rev. Lett.* **115**(4), 45501 (2015).
33. A. Meyer, J. Wuttke, W. Petry, A. Peker, R. Bormann, G. Coddens, L. Kranich, O. Randl, and H. Schober: Harmonic behavior of metallic glasses up to the metastable melt. *Phys. Rev. B. Condens. Matter* **53**(18), 12107 (1996).
34. A. Meyer, W. Petry, M. Koza, and M.-P. Macht: Fast diffusion in ZrTiCuNiBe melts. *Appl. Phys. Lett.* **83**(19), 3894 (2003).
35. F. Yang, T. Kordel, D. Holland-Moritz, T. Unruh, and A. Meyer: Structural relaxation as seen by quasielastic neutron scattering on viscous Zr–Ti–Cu–Ni–Be droplets. *J. Phys. Condens. Matter* **23**(25), 254207 (2011).
36. Z. F. Zhao, P. Wen, C. H. Shek, and W. H. Wang: Measurements of slow β -relaxations in metallic glasses and supercooled liquids. *Phys. Rev. B* **75**(17), 174201 (2007).
37. P. G. Debenedetti and F. H. Stillinger: Supercooled liquids and the glass transition.

- Nature* **410**, 259 (2001).
38. A. Heuer: Exploring the potential energy landscape of glass-forming systems: from inherent structures via metabasins to macroscopic transport. *J. Phys. Condens. Matter* **20**(37), 373101 (2008).
 39. A. Q. Tool: Relation between inelastic deformability and thermal expansion of glass in its annealing range. *J. Am. Chem. Soc.* **29**(9), 240 (1946).
 40. O. S. Narayanaswamy: A model of structural relaxation in glass. *J. Am. Ceram. Soc.* **54**(10) (1971).
 41. C. T. Moynihan, P. B. Macedo, C. J. Montrose, P. K. Gupta, M. A. DeBolt, J. F. Dill, B. E. Dom, P. W. Drake, A. J. Easteal, P. B. Elterman, R. P. Moeller, H. Sasabe, and J. A. Wilder: Structural relaxation in vitreous materials. *Ann. New York Acad. Sci.* **279**, 15 (1976).
 42. J. C. Maxwell: On the Dynamical Theory of Gases. *Philos. Trans. R. Soc. London.* **157**, 49 (1867).
 43. M. L. Lind, G. Duan, and W. L. Johnson: Isoconfigurational elastic constants and liquid fragility of a bulk metallic glass forming alloy. *Phys. Rev. Lett.* **97**, 15501 (2006).
 44. W. L. Johnson, M. D. Demetriou, J. S. Harmon, M. L. Lind, and K. Samwer: Rheology and Properties of Metallic Glass-Forming Liquids: A Potential Energy Landscape Perspective. *MRS Bull.* **32**(August 2007), 644 (2007).
 45. V. A. Khonik, Y. P. Mitrofanov, S. V. Khonik, and S. N. Saltykov: Unexpectedly large relaxation time determined by in situ high-frequency shear modulus measurements near the glass transition of bulk glassy Pd₄₀Cu₃₀Ni₁₀P₂₀. *J. Non. Cryst. Solids* **356**(23–24), 1191 (2010).
 46. H. Vogel: The law of the relationship between viscosity of liquids and the temperature. *phys. Z.* **22**, 645 (1921).

47. G. Fulcher: Analysis of recent measurements of the viscosity of glasses. *J. Am. Ceram. Soc.* **8**, 339 (1925).
48. G. Tammann and W. Hesse: Die Abhängigkeit der Viskosität von der Temperatur bei unterkühlten Flüssigkeiten. *Z. anorg. u. allg. Chem.* **156**, 245 (1926).
49. T. A. Vilgis: Strong and fragile glasses: A powerful classification and its consequences. *Phys. Rev. B* **47**(5), 2882 (1993).
50. R. Böhmer, K. L. Ngai, C. A. Angell, and D. J. Plazek: Nonexponential relaxations in strong and fragile glass formers. *J. Chem. Phys.* **99**(5), 4201 (1993).
51. I. M. Hodge: Enthalpy relaxation and recovery in amorphous materials. *J. Non. Cryst. Solids* **169**(3), 211 (1994).
52. G. W. Scherer: Use of the Adam-Gibbs Equation in the Analysis of Structural Relaxation. *J. Am. Ceram. Soc.* **67**, 504 (1984).
53. I. M. Hodge: Adam-Gibbs formulation of enthalpy relaxation near the glass transition. *J. Res. Natl. Inst. Stand. Technol.* **102**(2), 195 (1997).
54. B. Ruta, G. Baldi, Y. Chushkin, B. Rufflé, L. Cristofolini, A. Fontana, M. Zanatta, and F. Nazzani: Revealing the fast atomic motion of network glasses. *Nat. Commun.* **5**(May), 3939 (2014).
55. J. M. O'Reilly: Review of structure and mobility in amorphous polymers. *Crit. Rev. Solid State Mater. Sci.* **13**(3), 259 (1987).
56. S. L. Simon: Enthalpy Recovery of Poly(ether imide): Experiment and Model Calculations Incorporating Thermal Gradients. *Macromolecules* **9297**(14), 4056 (1997).
57. P. Bernazzani and S. L. Simon: Volume recovery of polystyrene: Evolution of the characteristic relaxation time. *J. Non. Cryst. Solids* **307–310**, 470 (2002).
58. S. L. Simon and P. Bernazzani: Structural relaxation in the glass: Evidence for a path dependence of the relaxation time. *J. Non. Cryst. Solids* **352**(42–49), 4763 (2006).

Figure Captions

FIG. 1: Diffraction intensity $I(q)$ measured on beam line ID15 at ESRF of the amorphous and partially crystalline (x-tal) samples of $\text{Zr}_{44}\text{Ti}_{11}\text{Ni}_{10}\text{Cu}_{10}\text{Be}_{25}$. The dashed curve highlights the difference between the two diffraction patterns.

FIG. 2: (a) Temperature dependence of $g_2(q_0, t)$ in partially crystallized $\text{Zr}_{44}\text{Ti}_{11}\text{Ni}_{10}\text{Cu}_{10}\text{Be}_{25}$ measured during step-cooling at a fixed $t_w = 7 \times 10^3$ s. Due to insufficient data at longer times, the data at 548 K are not fitted. (b) Evolution of the shape parameter β as a function of temperature and t_w . The data taken during cooling correspond to the partially crystalline sample; those during heating correspond to the fully amorphous sample.

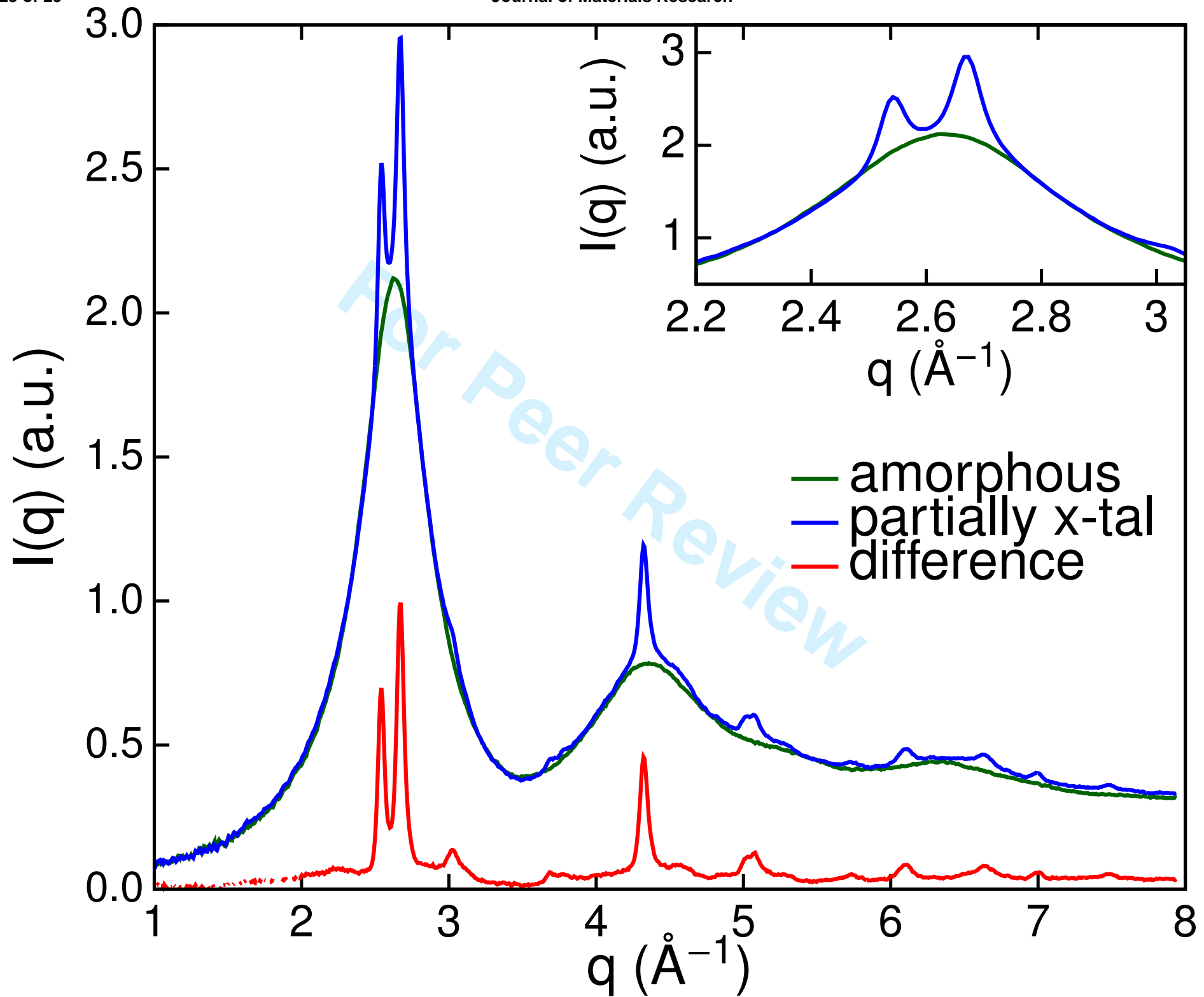
FIG. 3: Rescaled values of $g_2(q_0, t)$ show a clear (a) time-temperature superposition and (b) time-waiting time superposition, regardless of thermal protocol and structural state of the sample. The solid curves are fits to Eq. (2) with a $\langle \beta \rangle = 1.5$.

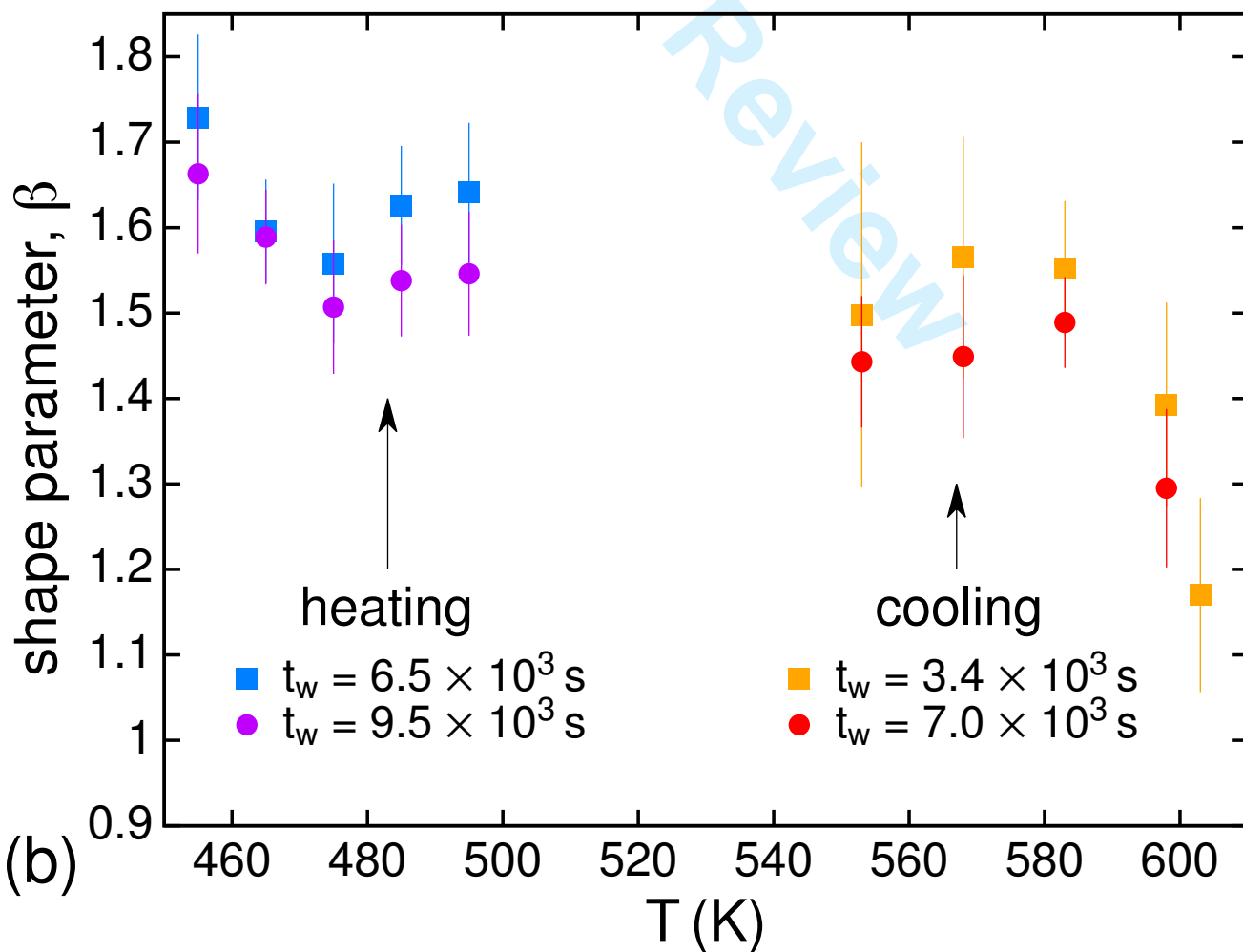
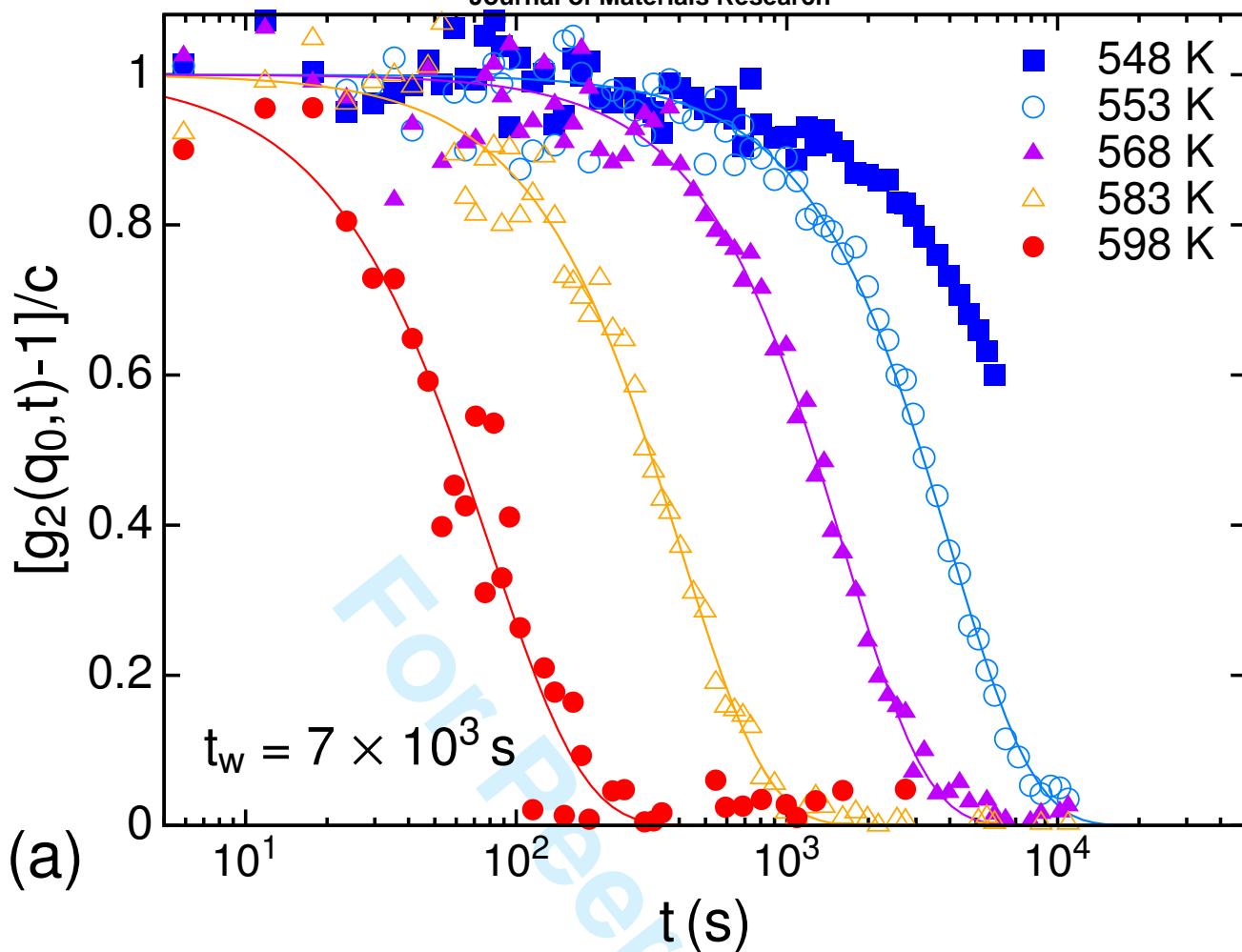
FIG. 4: XPCS structural relaxation times τ normalized to a temperature-dependent initial value of $\tau_I(T)$ as a function of t_w for all investigated temperatures. The waiting time dependence of $\tau/\tau_I(T)$ is well described by an empirical linear scaling law at all temperatures except 598 K. At this temperature, the microscopic dynamics of the glass do not evolve in time, similar to previous studies on a $\text{Pd}_{43}\text{Cu}_{27}\text{Ni}_{10}\text{P}_{20}$ BMG.¹¹

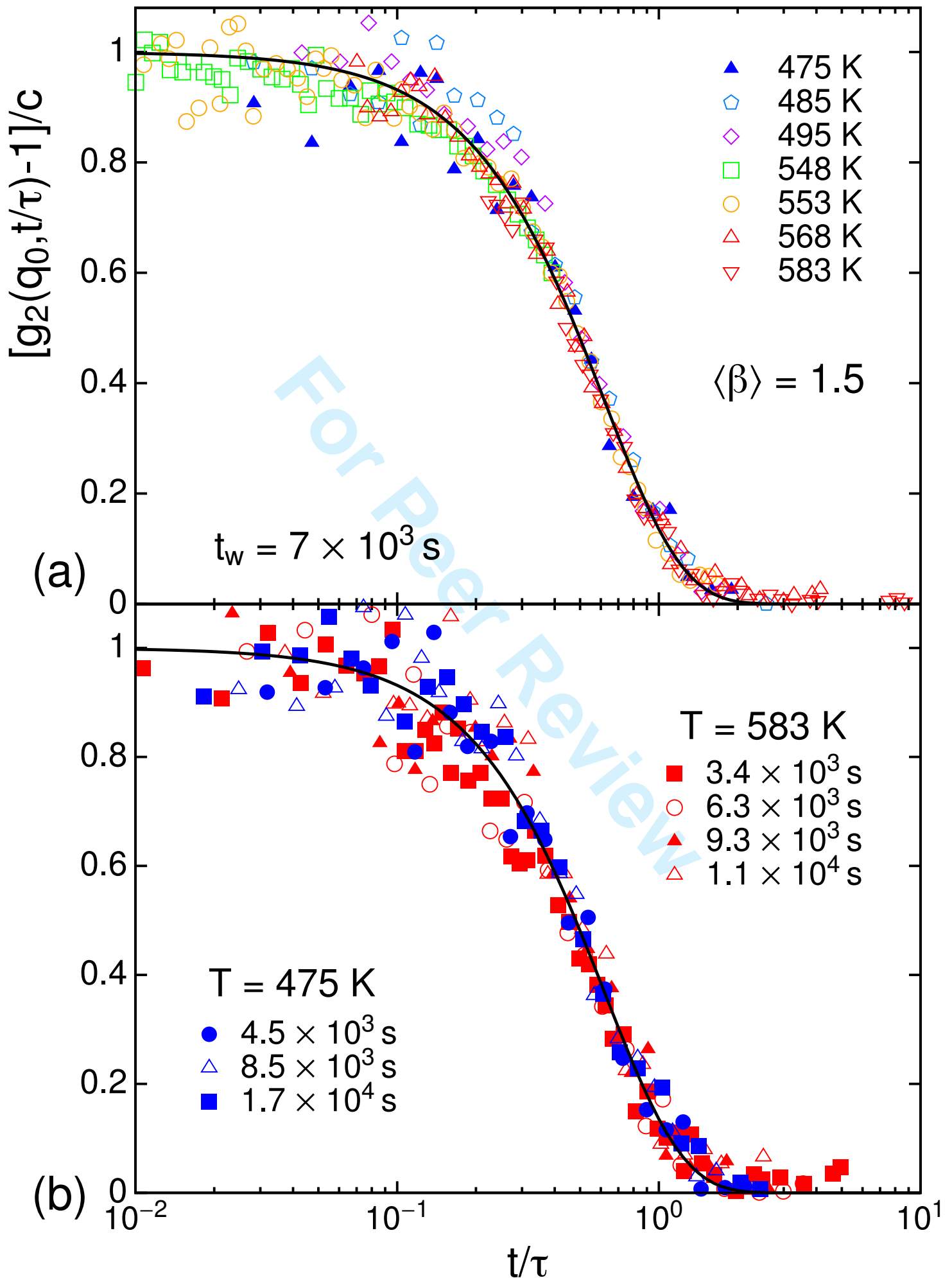
FIG. 5: Structural relaxation times τ of $\text{Zr}_{44}\text{Ti}_{11}\text{Ni}_{10}\text{Cu}_{10}\text{Be}_{25}$ as a function of inverse temperature. Equilibrium values in the supercooled liquid state were determined using DMA (filled circles). Equilibrium viscosities determined in beam-bending studies¹⁶ were re-scaled using Eq. (3) to obtain τ (filled squares). The dashed line is a fit of the equilibrium data to Eq.

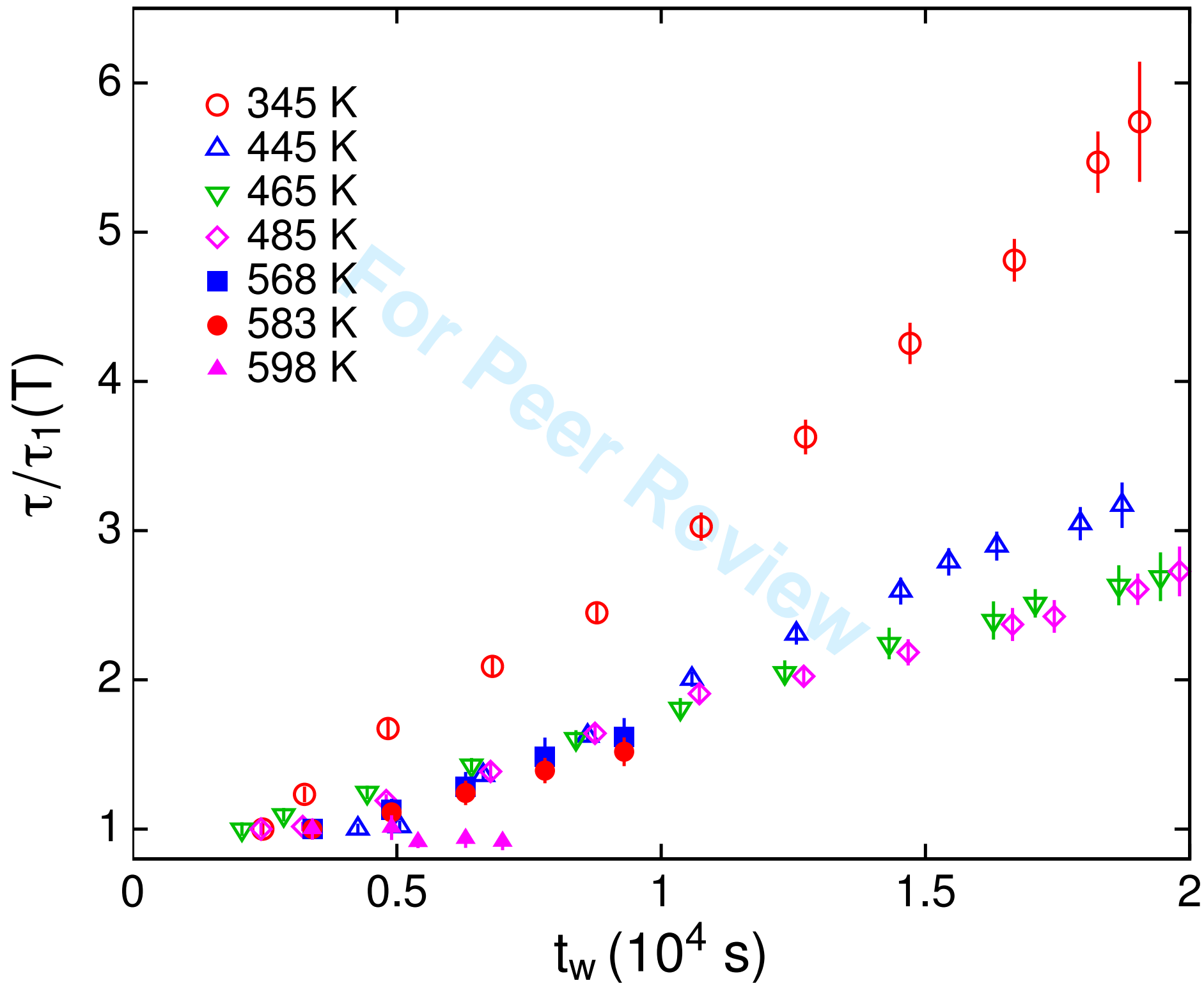
(4). Values in the glassy state are measured directly using XPCS (open triangles) and re-scaled from non-equilibrium viscosity values (filled triangles). The short-dashed lines are guides for the eye only. The solid line is the expected course of τ according to the Tool-Narayanaswamy-Moynihan model [Eqs. (5) and (6)].

1
2
3
4
5
6
7
8
9
10
11
12
13
14
15
16
17
18
19
20
21
22
23
24
25
26
27
28
29
30
31
32
33
34
35
36
37
38
39
40
41
42
43
44
45
46
47
48
49







1
2
3
4
5
6
7
8
9
10
11
12
13
14
15
16
17
18
19
20
21
22
23
24
25
26
27
28
29
30
31
32
33
34
35
36
37
38
39
40
41
42
43
44
45
46
47
48
49

